Wear Resistance of Gas Nitrided Astaloy CrL™ Sintered Steel

L. Alzati, U. Engström – Höganäs AB, Sweden
B. Rivolta, A. Tavasci – Politecnico di Milano, Lecco Campus, Italy

Abstract

Gas Nitriding treatment is proposed in combination with Shot Peening as a processing route to increase the wear performances of PM components made of prealloyed powder Astaloy CrL™. Porosity closure by surface densification allows limiting the depth of treatment and containing dimensional variations. 7,0 g/cm³ sintered density was considered.
Pin on disk tests have been carried out at a constant load of 5N, sliding distance up to 7500m and sliding speed in the range of 0,2-2m/s. Disks in both as-sintered and gas nitrided condition, with and without Shot Peening, have been tested against a WC static counterface. An energetic interpretation of the wear rates is here presented. The different surfaces have been initially characterized through macro and microhardness profiles, LOM observations, X-ray diffraction and texture analysis.

Introduction

It's known that for PM steels diffusion heat treatments are critical [1]. At nominal density close to 7,0 g/cm³, they are characterized by the presence of interconnected porosity, that is a dense network of intercommunicating pores. In presence of a diffusion heat treatment atmosphere, the core structure is therefore affected by diffusional phenomena too. Common Gas Nitriding treatment would allow the undesired development of compound layers even around the pores at the core of PM parts.
Dimensional variations are as well relevant matter in the case of PM parts manufacturing and low process temperatures can help limiting distortions and variations.
The result of a diffusion heat treatment is then strongly dependent on the interconnected porosity level and can't leave out of consideration an efficient control of process variables. In technical literature information on Ion Nitriding can be found, being the process not dependent on the open porosity and allowing a better control of the depth treatment. The ion process doesn't need a Nitriding atmosphere but provides a ion surface gunning.
The choice of Gas Nitriding of this study is related to the attempt to limit the process temperature and time and therefore its costs. Closing the open surface porosity by means of a densification technique allows containing the nitrided layer at the surface of PM parts. Correct setting of the treatment parameters require accurate control of the atomic nitrogen activity.
This paper compares the wear behaviour of the as-sintered material with the nitrided one, showing the benefits of the combination with Shot Peening.

Experimental procedures

The characterization of the wear resistance to sliding has been carried out for the Chromium and Molybdenum pre-alloyed powder Astaloy CrL™ -see chemical composition in Table 1.
Astaloy CrL™ was introduced as low alloyed alternative to Nickel, Copper and Molybdenum-based powders. It is characterized by high hardenability and various microstructures can be obtained adjusting the process parameters.

Cr [%wt]	Mo [%wt]
1,5	0,2

Table 1. Chemical composition of AstaloyCrL™.

The sintered material has been provided in the form of 9.85 mm nominal thickness and 40 mm nominal diameter disks at 7.0 g/cm^3 density –see Figure 1.

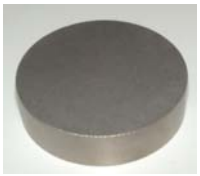

Figure 1. Sintered Disk.

The process parameters of the as-sintered condition are listed in Table 2. Microstructure has been observed by Light Electrical Microscopy (LOM); it consists of fine pearlite –see Figure 2 and Figure 3.

	Sintering parameters
Temperature	1120°C
Time	30min
Graphite	0,8%
Cooling rate	0,8°C/s
Atmosphere	N_2/H_2 90%/10%

Table 2. Sintering Parameters.

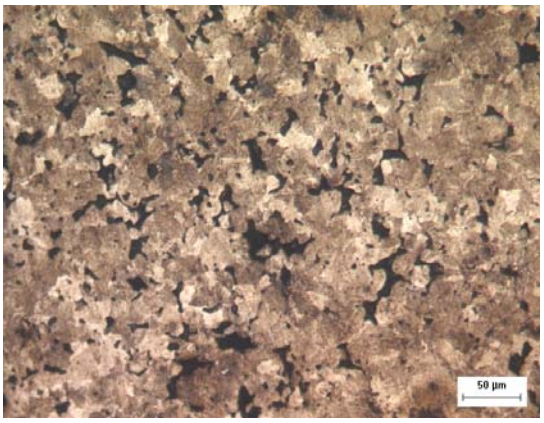

Figure 2. LOM. Overview of as-sintered disks' microstructure.

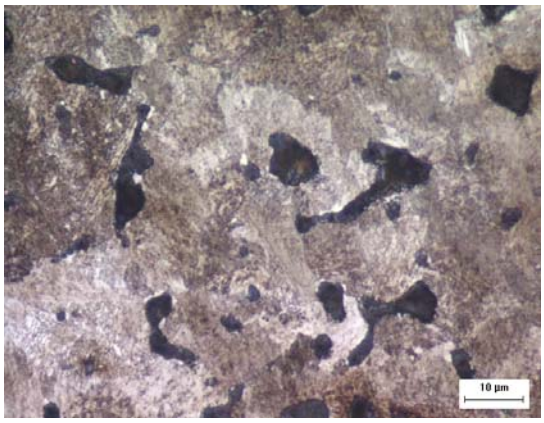

Figure 3. LOM. As-sintered disks' microstructure: fine pearlite.

Gas Nitriding process parameters have been optimised through previous experiments whose aim was to minimize the dimensional distortion and the development of a compound layer at the core structure [1]. Low process temperature and short soaking time in comparison to a classic Nitriding have been chosen –see Table 3.

Temperature	Time	Nitriding Potential
480 °C	1 h	1.2; 1.5

Table 3.Gas Nitriding parameters -see reference [1].

By following these Nitriding parameters, the core microstructure results similar to the as-sintered condition (Figure 4), but a white compound layer (white) can be observed down to a depth of some tenths of millimetre from the surface (Figure 5). At higher magnification, the development of a uniform white compound layer, that is absent at the core, can be seen all around the pores (Figure 6).

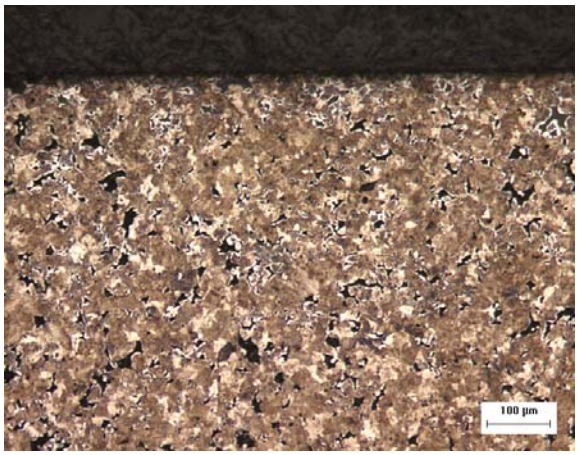

Figure 4. LOM. Overview of Gas nitrided disks' microstructure.

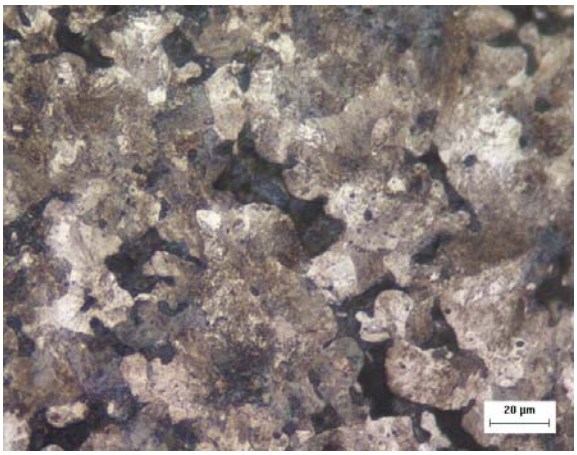

Figure 5. LOM. Gas nitrided disks' microstructure: fine pearlite.

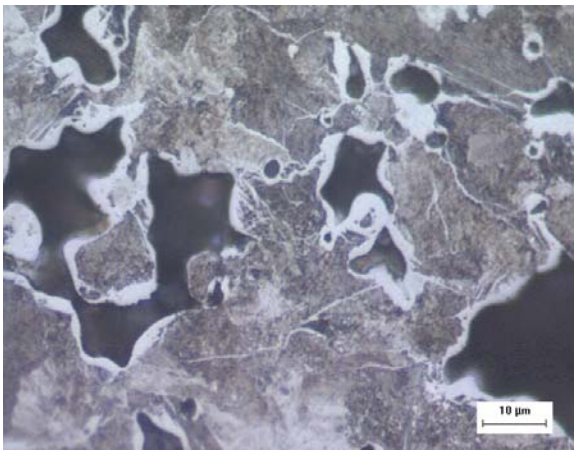

Figure 6. LOM. Gas nitrided disks' microstructure: compound layer, found at few tenths of millimetres below the surface.

The beneficial effect of the compound layer has been long debated: because of its high hardness value, it can be desired to enhance the wear resistance only if limited in extension to a defined surface layer.

Shot Peening is generally intended as a strain-hardening methodology. In this study the main goal was the sealing of the surface porosity, in order to insulate the core structure from the treatment atmosphere and therefore limit the Nitriding process to the surface layer only.

Shot Peening parameters have not been optimized for mechanical performance increase; Steel spheres of 100 µm diameter have been used for a time process equal to 8 minutes. Optimized Shot Peening paramenters for PM can be found in literature [2]. Figure 7 and Figure 8 are Scanning

Electron Microscopy (SEM) images of the as-sintered surface condition and the shot peened one respectively.

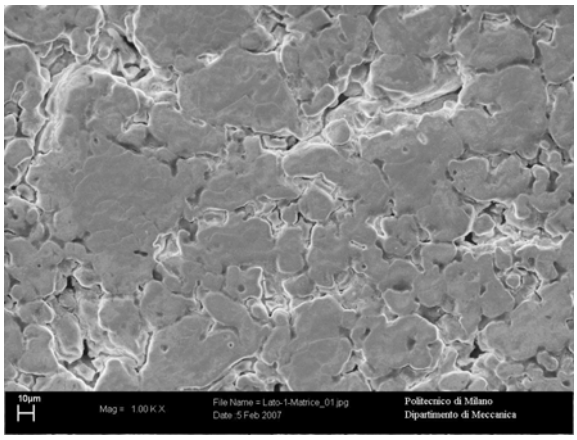

Figure 7. SEM. As-sintetered surface.

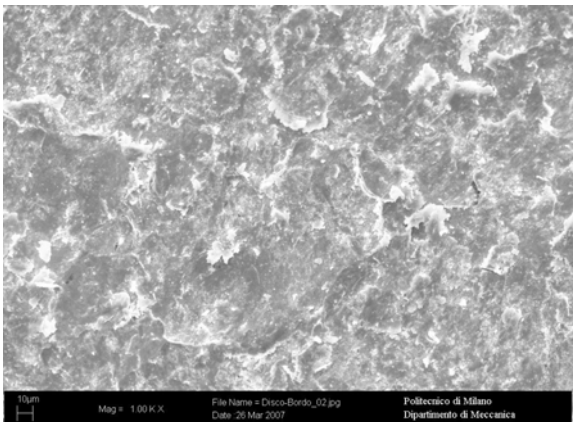

Figure 8. SEM. Shot peened surface.

LOM observations showed densified layer of about 60µm (Figure 9).

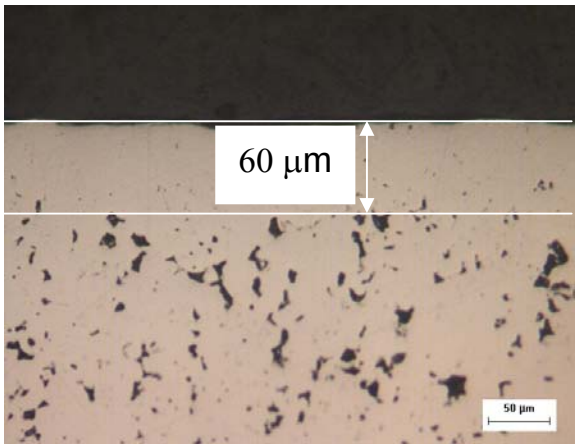

Figure 9. LOM. Densified surface layer after Shot Peening operations.

Gas Nitriding has been performed after Shot Peening adopting the same process parameters listed in Table 3. The LOM observation of the resulting microstructure leads to conclude that the effect of Nitriding is confined in a surface layer (Figure 10). No evidence of compound layer development is found below the densified layer (Figure 11).
Compared to the shot peened-only condition, a dimensional increase in thickness of about 0,05% has been recorded when Gas Nitriding was performed. Gas Nitriding after Shot Peening brings totally less than 0,1% dimensional change.
The characterization of the different surface conditions has been performed by means of microstructure analysis, macro and microhardness tests, residual stresses analysis and texture analysis. Wear resistance to sliding has been investigated by pin on disk tests.

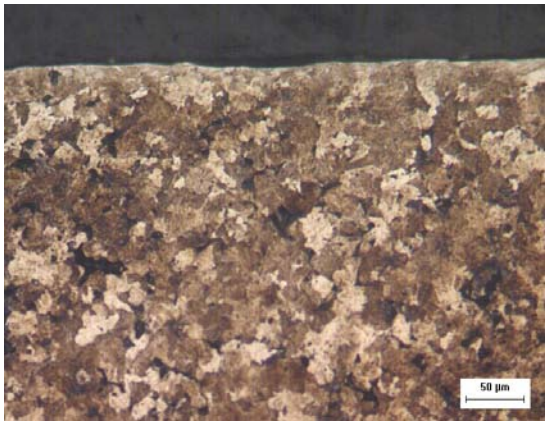

Figure 10. LOM. Overview of Shot Peened and Gas Nitrided disks' microstructure.

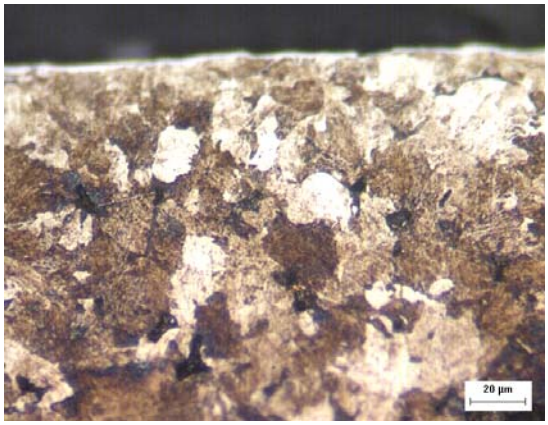

Figure 11. LOM. Microstructure of surface densified layer of Shot Peened and Gas Nitrided disks.

Sliding wear test in the "pin on disk" configuration have been carried out on a CSM Instruments tribometer (Figure 12). For all the tests the counterfacing material has been a sphere of tungsten carbide of 6 mm diameter, with a hardness of at least 1600 HV, representing the static partner. The wearable materials were the rotating disks of sintered steel. The evaluation of the wear rate has been done through measurements of the wear track at the profilometer and stereomicroscope observations for the correct interpretation of the wear process evolution [3, 4, 5].

Figure 12. Tribometer for pin on disk tests.

The tests have been conducted both in accordance to the standard ASTM – G99 (Rev. 05), that doesn't admit any test interruption and the evaluation of the wear track only at the end, and following an unconventional approach, allowing to analyse the contact geometry and the stresses at the interface and to give a correct interpretation of the wear mechanisms.
The surface finishing of the disks has been the same provided by the diffusion heat treatment in the former test. As for the identification of the wear mechanisms, the surface has been polished to exclude the effect of the surface texture, in the latter test. Table 4 summarizes the experimental conditions investigated as regards, the normal loads, the relative speed, the sliding distance and the track radius. The results have been before discussed following the Archard approach, and later reviewed in agreement with an energetic approach.

Normal Load [N]	1; 3; 5
Relative Speed [m/s]	0.2 – 2.0
Distance [m]	2000 – 7500
Track Radius [mm]	4 – 14.5

Table 4. Sliding wear tests parameters.

Through X-Ray Diffraction, the residual stress at the surface have been investigated. The analysis has been extended to a depth of 0,4 – 0,5 mm by means of electrochemical polishing, considering this value enough for giving a complete estimation of the profile of the residual stresses.

Results and Discussion

Hardness and surface characterization

Figure 13 shows the HV1 hardness profile obtained on the P/M steels after Nitriding, Shot-Peening and Shot Peening followed by Nitriding.
Results highlight that:

- On the as-nitrided sample, HV1 hardness profile shows effects of Gas Nitriding down to 2mm below the surface. Considering the effective treatment depth as the depth with an increase in hardness of at least 100 HV in comparison to the core structure, it can be estimated equal to 1 mm.
- Shot Peening didn't promote significant strain-hardening.
- The HV1 hardness profile after Shot Peening and Gas Nitrided disks is comparable the one after Shot Peening-only; this fact is mainly due to the fact that the macro scale doesn't allow highlighting any difference.

HV0,01 hardness profiles are shown in Figure 14. Significant difference among the processing routes is observed and effective case depth associated to Gas Nitriding treatment can be estimated: hardness gap between shot peened and gas nitrided versus shot peened-only can be traced from the surface down to a depth of roughly 70μm. Surface hardness values are nearly the same as for gas nitrided-only material.
The nitriding potential has been increased to 1.5 (about 25%), at constant process temperature and soaking time. The respective hardness profile shows beneficial effect of increased Nitriding potential: both effective depth of treatment and hardness values at the surface increase.
Figure 15 shows the complete microhardness profile on the as-nitrided samples.
HV0.01 hardness profile shows effects of Gas Nitriding down to 3mm below the surface, even though the effective layer is still close to 1 mm.

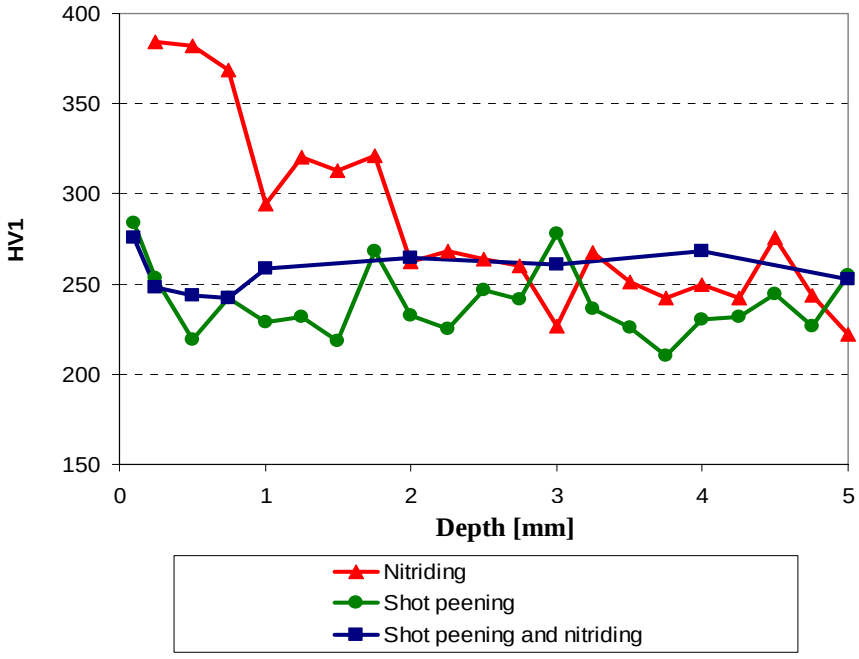

Figure 13. HV1 hardness profile after Gas nitriding, after Shot Peening and after Shot peening followerd by Gas Nitriding.

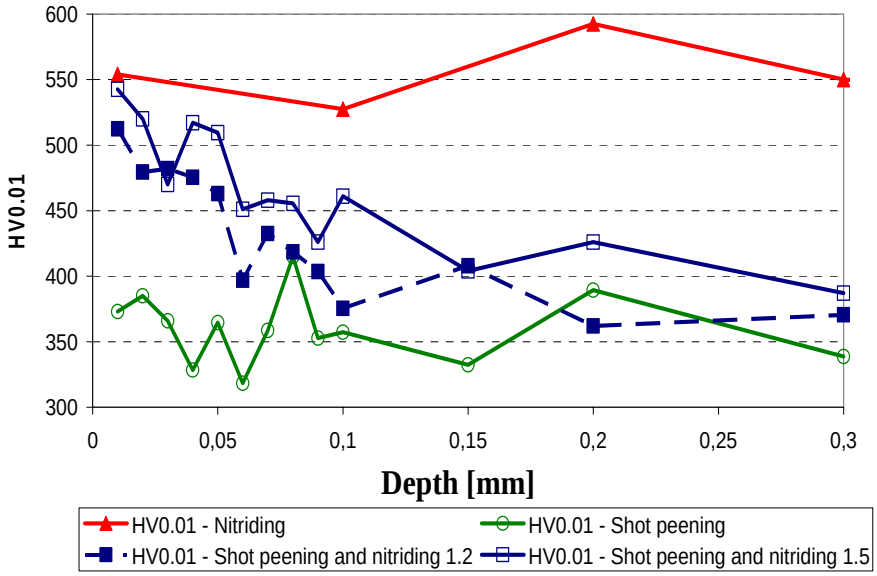

Figure 14. HV0.01 hardness profile after Gas nitriding, after Shot Peening and after Shot peening followed by Gas Nitriding.

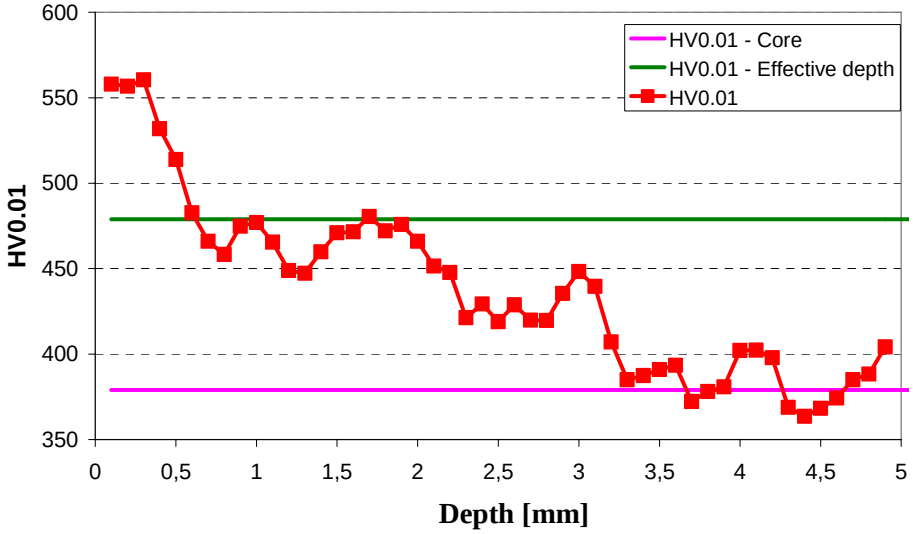

Figure 15. HV0.01 hardness profile after Gas nitriding.

Residual Stresses Analysis

The results of X-rays Diffraction analyses are plotted in Figure 6, comparing the condition of Gas Nitriding, Shot Peening and Shot Peening followed by Gas Nitriding. 1.2 Nitriding potential is here considered.

It is evident, as expected, that simple Gas Nitriding gives a constant compressive residual stress all along the effective depth of treatment, 50MPa the average value. More pronounced compressive residual stresses are observed for Shot Peening-only: a peak of -460MPa circa is achieved. As hardness profiles previously showed, the entity of the residual stresses did not strain-harden the material. Nitriding performed after Shot Peening leads instead to partial softening of the residual stresses coming from the Shot Peening: a peak of 230MPa circa is achieved as combination of Gas Nitriding and compressive residual stresses from Shot Peening. The inversion from compressive to tensile stresses shown in Figure is the result of the static equilibrium.

It can be concluded that the use of a densification technique in order to close the open porosity facing the surface of a PM part allows obtaining a defined case depth by Gas Nitriding.

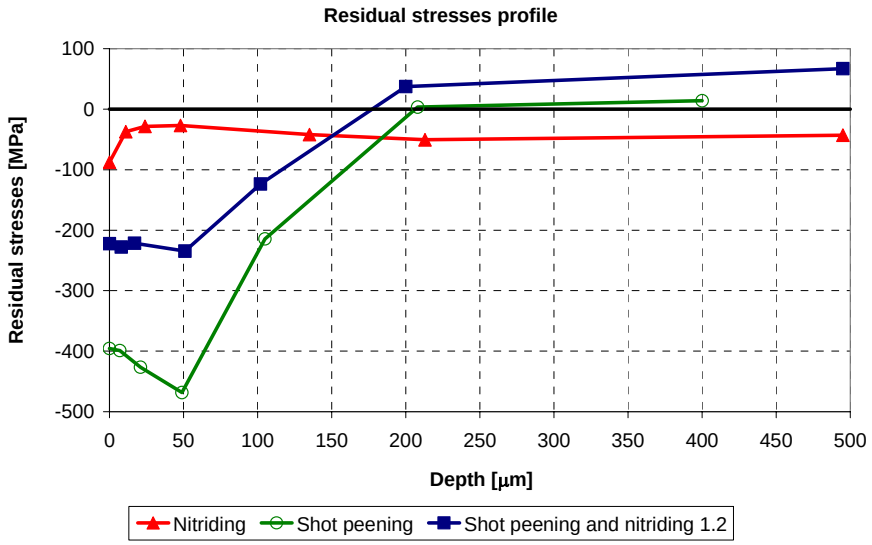

Figure 16. Residual stresses analysis (0-500µm) after Gas Nitriding, Shot Peening and Shot Peening followed by Gas Nitriding.

Surface roughness

Texture analysis has been run in order to give a complete characterization of the different conditions here investigated [3, 4].

The observation of the roughness profile in the as-sintered and shot peened conditions evidences a symptomatic difference. Figure 17 and Figure 18 are examples of the measured profiles, adopting the same magnification factor for both the horizontal and the vertical scale. Similar outcome is achieved by the comparison between surfaces after Gas Nitriding and after Shot Peening followed by Gas Nitriding.

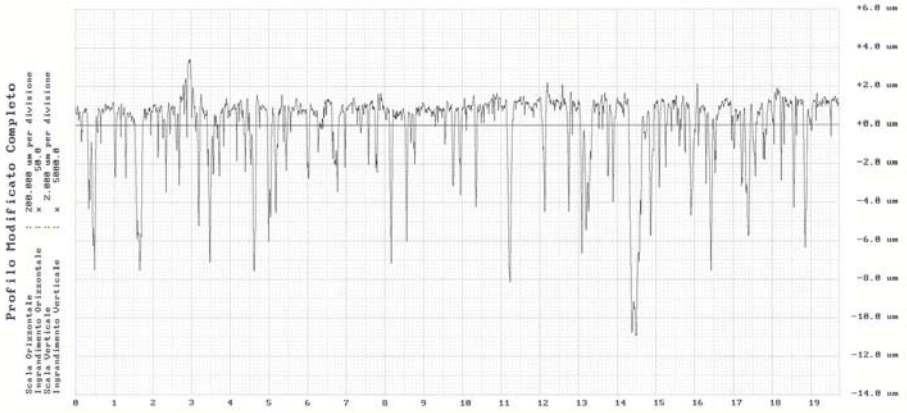

Figure 17. Roughness profile of as-sintered surface.

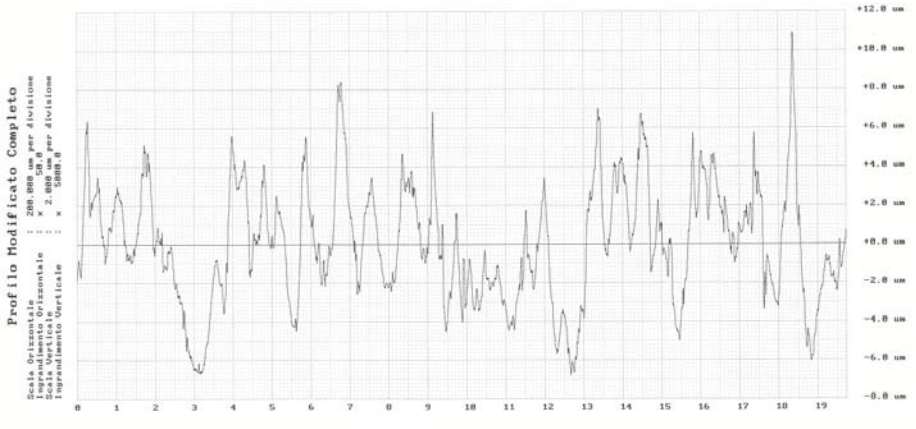

Figure 18. Roughness profile of shot peened surface.

For a better analysis of the surface texture, it is useful to define the following parameters:

- Material Ratio parameter - By considering a lapping plate resting on the highest peak of a profile (Figure 19), as the peaks wear and the bearing line descends down the profile, the length of the bearing line (the length of the profile in contact with the lapping plate) increases.

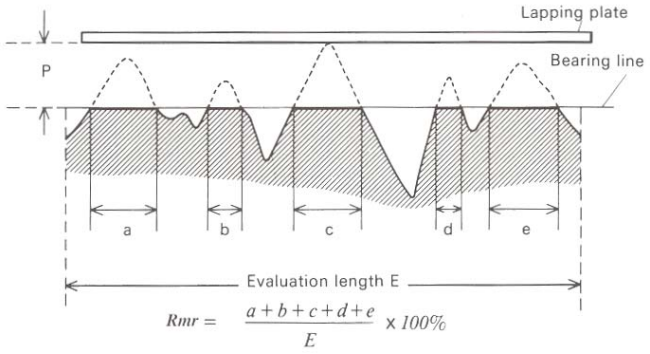

Figure 19. Material Ratio curve definition (see reference [13])

- Skewness and Kurtosis parameter. Considering that the surface profile can be described with a Gaussian distribution of the heights, these parameters are able to describe the shape of the distribution.

  The Skewness factor defines the asymmetry of the gaussian distribution (Figure 20): low/negative values (asymmetry on the left) represent a surface with hollows, whereas high/positive values (asymmetry on the right) denote the presence of protrusions.

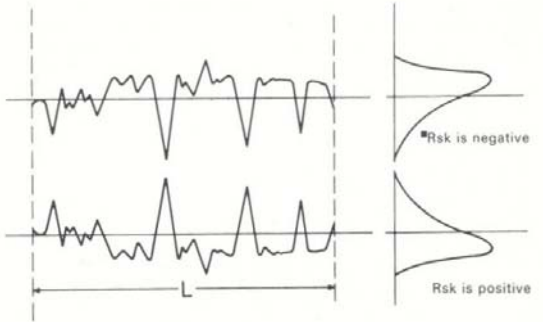

Figure 20. Meaning of Skewness factor R_{Sk} (see reference [13])

The Kurtosis factor is related to the flatness of the gaussian distribution: the flatter the Gaussian distribution, the lower the Kurtosis factor. Figure 21 shows the Material Ratio curve obtained from the analysis of the surface of the tested materials.

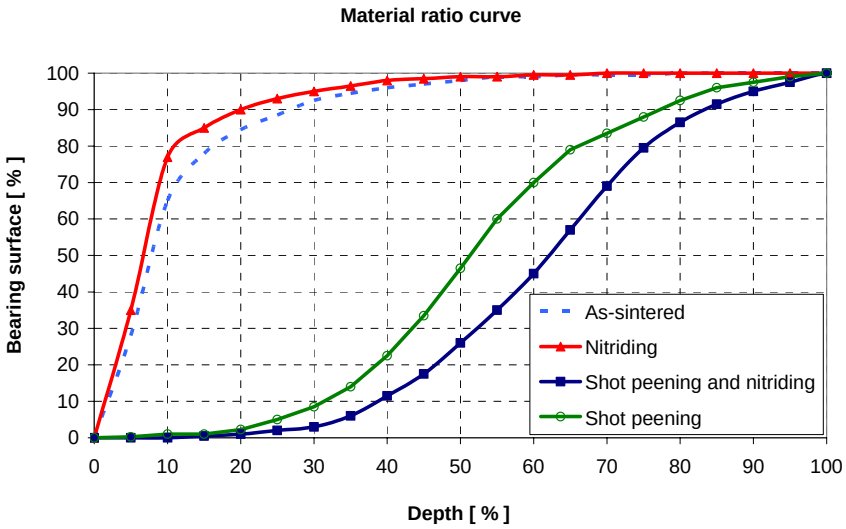

Figure 21. Material ratio curves, as defined in Figure, for all the surface conditions.

Strong discrepancy among material ratio curves is found when Shot Peening has been performed. In the Table 5 the obtained roughness index, the Skewness and Kurtosis factors are compared.

	As-sintered	Nitrided	Shot Peened	Shot Peened and Nitrided
R_a	1.19	1.18	1.86	2.10
R_{Sk}	-2.47	-2.21	0.1	-0.05
R_{Ku}	10.60	12.98	3.06	2.85

Table 5. Comparison of Roughness (Ra), Skewness (RSk) and Kurtosis (RSk) factors.

From the analysis of the charts, it's clearly verified that Shot Peening is discriminant for the surface morphology and that the Nitriding doesn't affect it. Shot Peening origins in fact subsidence on the external surface. Surface in the as-sintered condition or after gas nitrided are therefore morphologically similar, as well as the surface after Shot Peening and after Shot Peening followed by Gas Nitriding are comparable.

Wear resistance

The classic Archard approach states that the wear rate is the material loss per unit of load and unit of sliding distance [5, 6, 7]. According to this definition, a wear rate value can therefore be associated to each combination of experimental parameters. It's enough to interpolate with a straight line passing for the axis origin the loss volumes as a function of the product between normal load and sliding distance in order to extrapolate the angular coefficient, that is the wear rate. As shown in Figure 22, there's significant data dispersion for the as-sintered and the shot peened surface conditions. This fact underlines the limit of the classic theory for investigating the wear behaviour of materials that didn't undergo Gas Nitriding. This kind of approach doesn't consider that in a "pin on disk" test the contact pressure varies continuously admitting a wide range of stresses to which different wear mechanisms can correspond. A correlation between results of tests conducted under different experimental conditions of normal load, sliding speed, track radius and sliding distance is to be established.

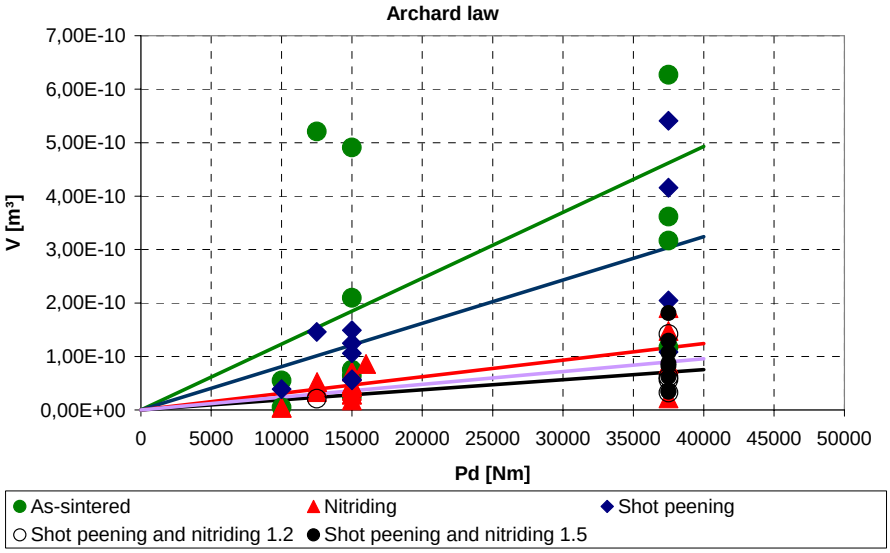

Figure 22. Wear tests results, interpreted through the Archard law.

The Archard interpretation allows however stating that the gas nitrided condition is the one with the highest wear resistance and that the correspondent wear rates are typical of a moderate wear regime. For the as-sintered and the shot peened surface condition, wear rates typical of transition mechanisms between a moderate wear regime and a severe one can be tracked, that is a high data dispersion according to Archard.

An energetic approach allows instead releasing the interpretation from the specific experimental conditions [8, 9, 10], by considering the normal load P and the sliding speed v, whose product is time constant and doesn't depend on the evolution of the contact geometry between rotating disk and static pin. The goal of the energetic approach is therefore to establish a correlation between wear rates and energy available for being spent in friction work. Considering the measured average value of the friction coefficient μ, the quantity $\mu P v$ is related to the friction work, responsible for the debris origin, the temperature increase in the contact region and the entropy increase because of the microstructure changes. The validity of an energetic approach is due to the fact that the results are properties of the material state and that they can be compared on the same graph not withstanding the differences in the experimental conditions.

Even from a first comparison between the as-sintered and the gas nitrided surface condition the excellence of an energetic approach for analysing the wear behaviour is highlighted: data fit well in a straight line on logarithmic scale, that is a power law. The ratio between the exponents of the power laws lets to estimate the gain due to the Gas Nitriding: 1,55. The exponent is in fact index of the wear rate increasing with the increasing of the energy input. In this case there is a strong divergence between the trends corresponding to the two surface conditions –see Figure 23.

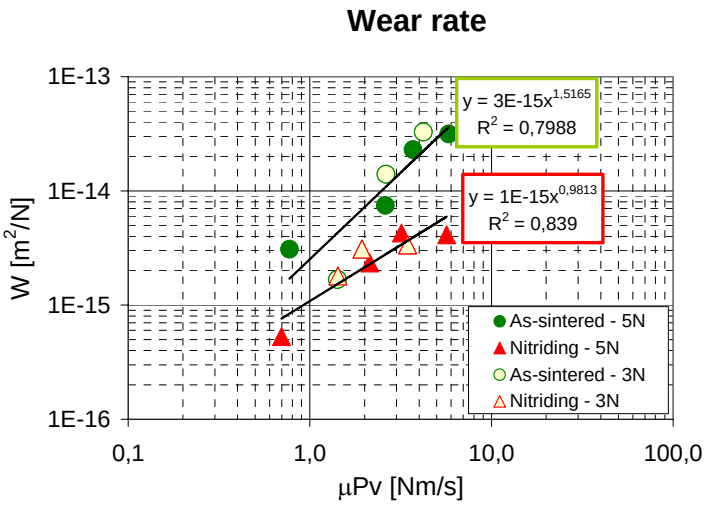

Figure 23. Wear tests results interpreted through the energetic approach for as-sintered and gas nitrided surface conditions.

Interposing a Shot Peening treatment between the as-sintered condition and the nitrided one, the ratio reaches a value of 2,55 and this is index of a major gain –see Figure 24. Analysing the results of the intermediate state of simply shot peened surface, it is evident that the Shot Peening reduces the slope of the data trendline, reducing the effect of stress amplification due to porosity. At the lowest value of energy input the wear rate are instead comparable. Gas Nitriding performed after Shot Peening reduces then the wear rates of about one magnitude order.

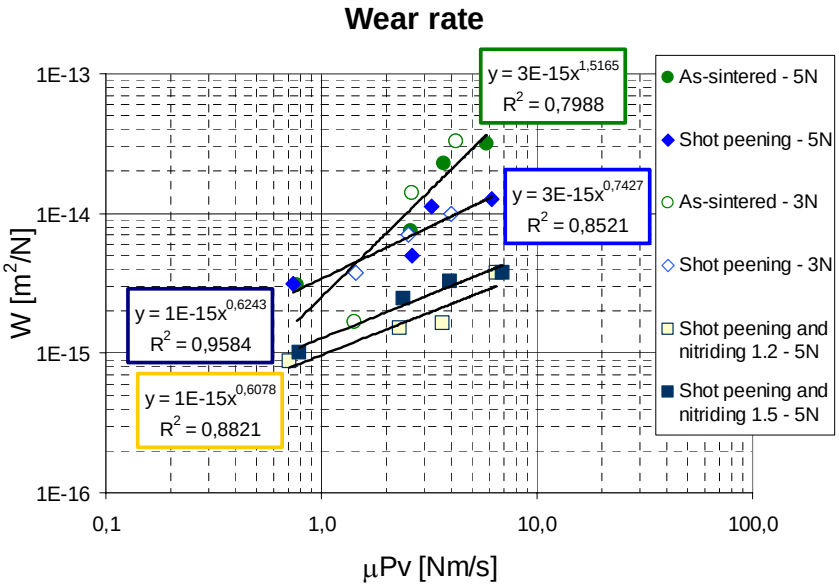

Figure 24. Wear tests results interpreted through the energetic approach for as-sintered surface, after Shot Peening and after Shot Peening followed by Gas Nitriding.

Non-standard wear tests have been performed. Pin on disk tests were carried out at the lowest sliding speed in order to minimize the induced vibrations and they were interrupted at different intermediate steps of sliding distance: at each step the wear rate was evaluated by measurements at the profilometer and the contact pressures estimated by stereo microscope analysis. The aim of

these tests was to generate a curve of the wear rate as a function of the contact pressure as a property of the microstructure of the steel.
Moreover, the surface of each tested disk was polished in order to test the wear behaviour of the microstructure with no influence of the surface roughness. It is well known that it is a useful test for the evaluation of the resistance of material to galling [10, 11, 12].
On the pin surface the extension of the contact area was easy to be estimated. A punctual curve of the wear rate as a function of the nominal contact pressure was built for each material condition.
The results are plotted in Figure 25, where it can be seen that:

- The wear rates in the severe wear regime are similar for the as-sintered and the as-nitrided sample.
- The transition from a mild to a severe wear regime occurs at lower contact pressure in the as-sintered than in the as-nitrided state.

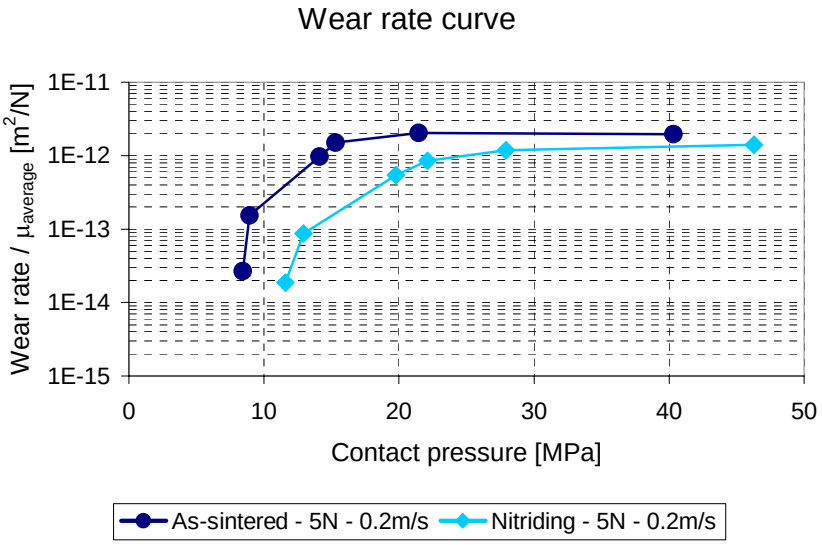

Figure 25. Wear rate curve.

Conclusions

Gas Nitriding can successfully be performed on surface densified PM parts: in this study evidence was given of controlled nitrided layer on shot peened Astaloy CrL^{TM} disks.
By the combination of Shot Peening and Nitriding:

- Less than 0.1% dimensional change was observed.
- Highest wear resistance was shown in moderate wear regime (10^{-15}-10^{-14} m^2/N) as well as under the highest load, in comparison to as-sintered, shot peened-only and gas nitrided-only surfaces.

References

1. "*Composition and morphology of Fe-N off-equilibium phases in a nitrided Fe-1.5wt.%Mo sintered alloy*", M.R: Pinasco, G. Palombarini, M.G. Ienco, G.F. Bocchini, Journal of Alloy and Compounds 220 (1995), pp. 217 – 224.
2. *"Influence of secondary operations on mechanical properties of low alloyed sintered steel"*, K. Kanno, A. Bergmark, L. Alzati *et al*., PM World Congress 2004, Wien (Austria), 2004.

3. "*Friction, Wear, Lubrication – A textbook in Tribology*", Kenneth C Ludema, CRC Press, 1996.
4. "*Friction, Lubrication and Wear Technology*", ASM Handbook Vol. 18, ASM International, 1992.
5. "*The relationship between wear and dissipated energy in sliding systems*", A. Ramalho, J.C. Miranda, Wear 260 (2006), pp. 361 – 367.
6. "*The significance and use of the friction coefficient*", Peter J. Blau, Tribology international 34 (2001), pp 585 – 591.
7. "*Simultaneous observation of the evolution of debris density and friction coefficient in dry sliding steel contacts*", I. Sherrington, P. hayhurst, Wear 249 (2001), 182 – 187;
8. "*On the nature of running in*", Peter J. Blau, Tribology International 38 (2005), pp. 1007 – 1012.
9. "*Modelling and simulation of wear in a pin on disc tribometer*", V. Hegadekatte, N. Huber and O. Kraft, Tribology Letters, Vol. 24, No. 1, October 2006.
10. "*A test methodology for the determination of wear coefficient*", L.J. Yang, Wear 259 (2005), pp 1453 – 1461.
11. "*Influence of wear particle interaction in the sliding interface on friction of metals*", D.H. Hwang, D.E. Kim, S.J. Lee, Wear 225 – 229 (1999), pp. 427 – 439.
12. "*Simultaneous observation of the evolution of debris density and friction coefficient in dry sliding steel contacts*", I. Sherrington, P. Hayhurst, Wear 249 (2001), pp. 182 – 187.
13. Exploring Surface Texture, *Taylor Hobson Handbook*, 1998